Theoretical study of nuclear charge densities with elastic electron scattering

Yanyun Chu (褚衍运),[1,*] Zhongzhou Ren (任中洲),[1,2] Tiekuang Dong (董铁矿),[1,3] and Zaijun Wang Wang (王再军)[1,4]

[1]*Department of Physics, Nanjing University, Nanjing 210008, People's Republic of China*

[2]*Center of Theoretical Nuclear Physics, National Laboratory of Heavy-Ion Accelerator, Lanzhou 730000, People's Republic of China*

[3]*Macau University of Science and Technology, Macau 999078, People's Republic of China*

[4]*Department of Mathematics, Physics and Information Science, Tianjin University of Technology and Education, Tianjin 300222, People's Republic of China*

(Received 5 February 2009; published 21 April 2009)

The calculated cross sections for elastic Coulomb electron scattering from the phase-shift analysis method and the eikonal approximation are compared. It is shown that the phase-shift analysis method can reproduce the experimental data very well for both light and heavy nuclei. Then the phase-shift analysis is used to investigate elastic electron scattering along the O and S isotopic chains, where the charge densities are obtained from relativistic mean-field theory. Results show that the minima of the differential cross section shift inward and upward with the increase of the neutron number.

DOI: 10.1103/PhysRevC.79.044313 PACS number(s): 25.30.Bf, 21.10.Ft, 21.60.−n

I. INTRODUCTION

High-energy elastic electron scattering is a clear and precise tool for probing nuclear structure, in particular, nuclear charge densities [1,2]. It has been about half a century since the pioneering study of electron scattering on atomic nuclei by Hofstadter *et al.* [3–5]. Since then, a lot of work in this area has been done, and many valuable and precise data on the nuclear electromagnetic properties have been accumulated [6–8]. However, owing to the limitation of the techniques of making targets, electron scattering experiments were mainly carried out for stable nuclei in the past [9–11].

These days, it is important and exciting to explore the properties of the exotic nuclei in both experiment and theory. With the development of Radioactive Ion Beam (RIB) facilities, we are now able to produce some exotic nuclei with short half-lives and investigate their properties in the laboratory [12–15]. Many exotic properties, such as proton halos, neutron halos, and new magic numbers, have been discovered, all of which are relevant to nuclear density distributions. Up to now, the density distributions of exotic nuclei have been mainly obtained from nucleus-nucleus collisions, and the explanations of such experimental data are model dependent. To get precise nuclear charge densities, elastic electron scattering off exotic nuclei must be obtained experimentally. Experimental facilities for this purpose are now under construction at RIKEN and GSI [16–19]. In the near future, elastic electron scattering off exotic nuclei will be realized. Thus, at present, it is interesting and necessary to study electron scattering off exotic nuclei theoretically to provide the future experiments with some useful instructions in advance.

There are several theoretical methods used to study elastic electron-nucleus scattering, such as the plane-wave Born approximation (PWBA), the eikonal approximation, and the phase-shift analysis method [20–22]. The PWBA method can give qualitative results and has been used widely for its simplicity. To include the Coulomb distortion effect, which is neglected in PWBA, the other two methods may be used. In the past few years, some theoretical studies of elastic electron scattering off exotic nuclei have been performed. Wang *et al.* [23–25] studied such scattering along some isotopic and isotonic chains by combining the eikonal approximation with relativistic mean-field (RMF) theory. Antonov *et al.* [26,27] studied electron scattering from some unstable neutron-rich nuclei in the shell model and the Skyrme HF+BCS method. And, very recently, Roca-Maza *et al.* [28] systematically investigated elastic electron scattering off both stable and exotic nuclei with the phase-shift analysis method.

Although much work has been devoted to elastic electron-nucleus scattering recently [23–30], little has been done about the comparison among the calculated results from different scattering methods. It is interesting to note that Murphy and Überall [31] have compared the difference of the eikonal approximation, Born approximation, and the phase-shift analysis. Furthermore, there remain numerous important isotopes that have not been covered in previous theoretical investigations. Thus, in this article, we will compare the numerical results from the eikonal approximation and the phase-shift analysis method where the charge densities take the Fermi or three-parameter Fermi (3pF) form. After that, we will systematically study elastic electron scattering off the O and S isotopic chains by combining the phase-shift analysis method with RMF theory.

This article is organized as follows. In Sec. I, two methods for elastic electron scattering are briefly introduced. In Sec. III, we compare the results from the two different methods and calculate the differential cross sections of elastic electron scattering off some O and S isotopes. Finally, a summary is given.

II. THEORY

The elastic electron scattering process can be described by the Dirac equation [20]

$$[\alpha \cdot \mathbf{p} + \beta m + V(r)]\Psi(\mathbf{r}) = E\Psi(\mathbf{r}), \tag{1}$$

*chuyanyun@gmail.com

where α and β are the Dirac matrices, E and $\mathbf{p}$ are the energy and momentum of the incident electrons, respectively, m is the rest mass of the electron, and $V(r)$ is the potential between the electron and the nucleus, which is assumed to be a Coulomb potential here.

To obtain the differential cross section of the elastic electron scattering, we should solve this Dirac equation. In the following we briefly introduce two methods: phase-shift analysis and the eikonal approximation. These two methods are both standard methods for elastic electron scattering, so we will only outline them here.

A. Phase-shift analysis

In the Dirac equation, $V(r)$ is a spherical scalar potential. Therefore, the wave function can be expanded in terms of a series of spherical spinors with definite angular momenta [32]

$$\Psi(\mathbf{r}) = \frac{1}{r}\begin{bmatrix} P(r)\Omega_{\kappa,m_j}(\theta,\phi) \\ i\,Q(r)\Omega_{-\kappa,m_j}(\theta,\phi) \end{bmatrix}, \tag{2}$$

where $P(r)$ is the upper component radial wave function, $Q(r)$ is the lower component one, and Ω are the spherical spinors. The functions $P(r)$ and $Q(r)$ satisfy

$$\begin{aligned} \frac{dP}{dr} &= -\frac{\kappa}{r}P(r) + [E - V(r) + 2m]Q(r), \\ \frac{dQ}{dr} &= -[E - V(r)]P(r) + \frac{\kappa}{r}Q(r). \end{aligned} \tag{3}$$

Having determined the asymptotic behavior of $rV(r)$, we can express the upper and lower radial wave functions at large distances as

$$\begin{aligned} P(r) &= F^{(u)}(r)\cos\delta + G^{(u)}(r)\sin\delta, \\ Q(r) &= F^{(l)}(r)\cos\delta + G^{(l)}(r)\sin\delta, \end{aligned} \tag{4}$$

where $F^{(u,l)}$ and $G^{(u,l)}$ are the regular and irregular Dirac spherical Coulomb functions, the signatures u and l stand for the upper and lower components, and δ is the phase shift.

By solving the coupled radial equations [Eqs. (3)] with the asymptotic behavior defined in Eqs. (4), we can get the spin-up (δ_l^+) and spin-down (δ_l^-) phase shifts for the partial wave with orbital angular momentum l. Then we can determine the direct scattering amplitude

$$f(\theta) = \frac{1}{2ik}\sum_{l=0}^{\infty}[(l+1)(e^{2i\delta_l^+} - 1) + l(e^{2i\delta_l^-} - 1)]P_l(\cos\theta) \tag{5}$$

and the spin-flip scattering amplitude

$$g(\theta) = \frac{1}{2ik}\sum_{l=0}^{\infty}[e^{2i\delta_l^-} - e^{2i\delta_l^+}]P_l^1(\cos\theta), \tag{6}$$

where P_l and P_l^1 are the Legendre polynomials and associated Legendre functions, respectively. The differential cross section for elastic electron-nucleus scattering can be obtained as follows:

$$\frac{d\sigma}{d\Omega} = |f(\theta)|^2 + |g(\theta)|^2. \tag{7}$$

B. Eikonal approximation

The starting point of the eikonal approximation is a modulated plane-wave spinor [22–25]

$$\Psi(\mathbf{r}) = \Phi(\mathbf{r})u_0(\mathbf{k}_0)e^{i\mathbf{k}_0\cdot\mathbf{r}}, \tag{8}$$

where $u_0(\mathbf{k}_0)e^{i\mathbf{k}_0\cdot\mathbf{r}}$ describes a plane wave with momentum $\mathbf{k}_0$ and the modulating function $\Phi(\mathbf{r})$ is a 4×4 matrix operator.

Applying standard scattering theory and choosing the cylindrical system with z axis along the direction of the incident electrons, we can obtain the differential cross section

$$\frac{d\sigma}{d\Omega} = \cos^2\frac{\theta}{2}|I(q)|^2, \tag{9}$$

where θ is the scattering angle, q is the momentum transfer, and $I(q)$ is the scattering amplitude, which takes the form

$$I(q) = -ik\int_0^{+\infty} J_0(qb)[e^{i\chi(b)} - 1]bdb. \tag{10}$$

In the integral of Eq. (10), J_0 is the Bessel function and $\chi(b)$ is the eikonal phase-shift function

$$\chi(b) = -\frac{E}{k}\int_{-\infty}^{+\infty} V(r)dz, \tag{11}$$

where $r = \sqrt{z^2 + b^2}$ and b is the impact parameter.

On the whole, the eikonal approximation is based on the assumption that the interaction changes slowly enough so that the local momentum $\hbar k(\mathbf{r})$ ($\hbar k(\mathbf{r}) = \sqrt{2m[E - V(\mathbf{r})]}$) is nearly constant over many wavelengths [33]. For high-energy electron-nucleus scattering, the wavelength is very tiny, and the variation of the Coulomb interaction between the electron and the nucleus over many wavelengths is very small compared with the scattering energy. Thus the local momentum of the electron almost remains constant over many wavelengths, and therefore the eikonal approximation is suitable for high-energy electron scattering.

III. NUMERICAL RESULTS AND DISCUSSION

In this section, our task is twofold. First, we compare the results from the eikonal approximation and the phase-shift analysis method. Second, we calculate the differential cross sections of electron scattering off some O and S isotopes.

A. Comparison of results from the eikonal approximation and the phase-shift analysis

For high-energy (about several hundred MeV) elastic electron scattering, the eikonal approximation is assumed to be a good choice for its simplicity and directness in physical treatment [22]. Wang *et al.* [23–25] have generalized the eikonal approximation to study elastic electron scattering off proton-rich and neutron-rich nuclei. It has been pointed out that the nuclear charge form factor from elastic electron scattering can reflect some exotic properties of proton-rich nuclei. Recently, Roca-Maza and co-workers [28,34] have modified their published code ELSEPA to study elastic electron-nucleus scattering with the phase-shift analysis method. In this section,

TABLE I. Parameters of the charge distributions for ^{208}Pb, ^{118}Sn, ^{32}S, and ^{16}O.

	w	c	z	Reference
^{208}Pb (250 MeV)	0.62	6.25	0.58	[35]
^{208}Pb (502 MeV)	0	6.64	0.53	[36]
^{118}Sn	0	5.412	0.560	[37]
^{32}S	−0.213	3.441	0.624	[38]
^{16}O	−0.051	2.608	0.513	[39]

we will choose ^{208}Pb, ^{118}Sn, ^{32}S, and ^{16}O as examples to compare the calculated results from these two methods.

First, we study ^{208}Pb. The differential cross sections of elastic electron scattering off ^{208}Pb at 250 MeV were measured and the charge density of ^{208}Pb was fitted with the 3pF distribution [35]

$$\rho_c(r) \propto \frac{1 + wr^2/c^2}{1 + e^{(r-c)/z}}, \tag{12}$$

where the three parameters are w, c, and z. The fitted values of the parameters for ^{208}Pb are listed in Table I. With the parametrized nuclear charge density, we can determine the interaction between the electron and the target nucleus. Then we can obtain the differential cross sections by solving the Dirac equation with different methods. Figure 1 shows the differential cross sections calculated with the eikonal approximation and the phase-shift analysis. It is seen from Fig. 1 that the phase-shift analysis gives a good description of elastic electron scattering off ^{208}Pb at 250 MeV. For a large range of momentum transfer, the results from the phase-shift analysis agree well with the experiment. The differential cross section curve calculated from the eikonal approximation has the same shape as that from the phase-shift analysis, and the positions of the diffraction minima and maxima from these two methods are almost the same. But the differential cross section curve from the eikonal approximation is shifted slightly downward as a whole, especially at large momentum transfers.

Figure 2 shows the differential cross sections of elastic electron scattering off ^{208}Pb at 502 MeV. The experimental data are taken from Ref. [36]. It is clear that the cross sections can be reproduced very well by both the phase-shift method and the eikonal approximation, and the difference between the results from these two methods are smaller compared with the results at 250 MeV. This means that the phase-shift method is applicable to both low and high energy and that the eikonal approximation becomes more and more precise with increasing incident energy.

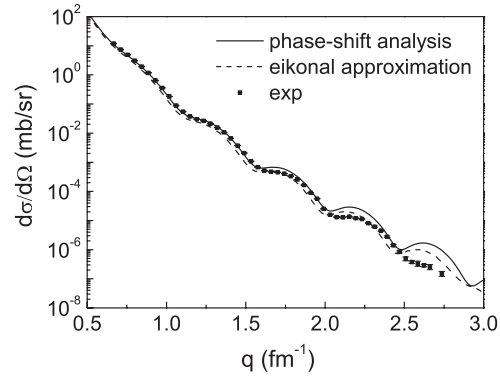

FIG. 2. Elastic electron scattering off ^{208}Pb at 502 MeV.

Calculations for 225-MeV elastic electron scattering off ^{118}Sn are also performed, and the results are shown in Fig. 3. The experimental data are taken from Ref. [37]. Comparing with Fig. 1, we find that the difference between the results from the two methods becomes smaller for this lighter nucleus.

Similar calculations are carried out for ^{32}S at 250 and 500 MeV, respectively. Figure 4 shows the results for ^{32}S at 250 MeV, and Fig. 5 shows the results at 500 MeV. The experimental differential cross section data and the parameters of the 3pF charge distribution are taken from Ref. [38]. From Figs. 4 and 5, we can also identify the downward shift of the eikonal results between the first and second diffraction minimum, comparing with the differential cross section curve from the phase-shift analysis. But the results from the two methods at small momentum transfers (i.e., inside the first diffraction minimum) are almost the same. The difference between the results from these two methods for ^{32}S is less distinct than those for ^{208}Pb and ^{118}Sn, indicating that the eikonal approximation is more suitable for the light nuclei. This is because the eikonal approximation takes into account the Coulomb distortion effects in a coarse way compared with the phase-shift analysis method. For the lighter nucleus, the Coulomb interaction between the electron and the nucleus is weaker. Thus the variation of this interaction

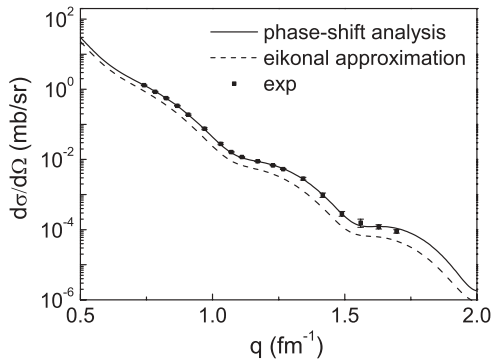

FIG. 1. Elastic electron scattering off ^{208}Pb at 250 MeV.

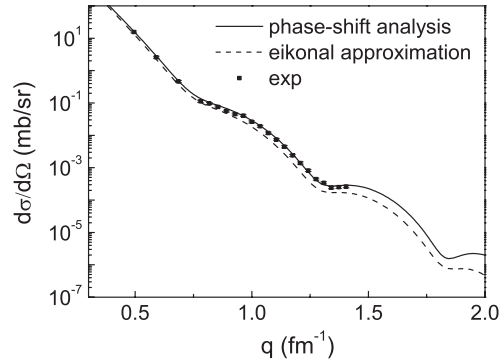

FIG. 3. Elastic electron scattering off ^{118}Sn at 225 MeV.

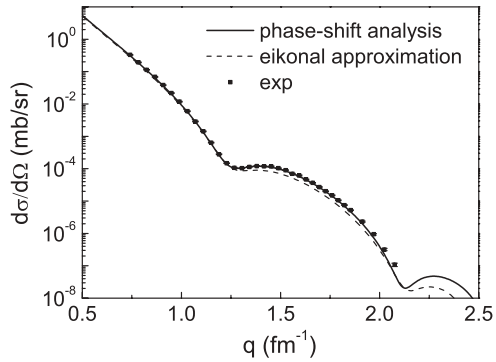

FIG. 4. Elastic electron scattering off ^{32}S at 250 MeV.

is smoother and the eikonal approximation can treat the Coulomb distortion effects with better accuracy. Conversely, for the heavier nucleus, the Coulomb interaction is stronger, the interaction potential varies more rapidly, and the accuracy of the eikonal approximation becomes lower. Comparing the results for ^{32}S at 250 and 500 MeV, we find that the difference between the results from the two methods at 500 MeV is even smaller. This also confirms that it is more appropriate to use the eikonal approximation for higher energy electron scattering.

Figure 6 shows the differential cross section of 374.5-MeV elastic electron scattering off ^{16}O. The experimental data and 3pF parameters are taken from Ref. [39]. The 3pF distribution parameters are specified in Table I. Comparing the results with those of ^{208}Pb, ^{118}Sn, and ^{32}S, we find that the difference resulting from the two methods is hard to identify for ^{16}O. Both of the methods can well reproduce the experimental data of ^{16}O.

According to these calculations, we can see that the numerical results from the phase-shift analysis are in good agreement with the experimental data within the considered range of momentum transfers. This is not a coincidence. From the theoretical point of view, the phase-shift analysis is a method based on exactly solving the Dirac equation with scattering boundary conditions. Thus it can well reproduce the experimental data in a wide range of scattering energy

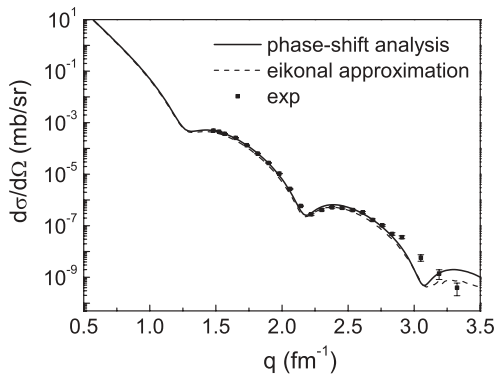

FIG. 5. Elastic electron scattering off ^{32}S at 500 MeV.

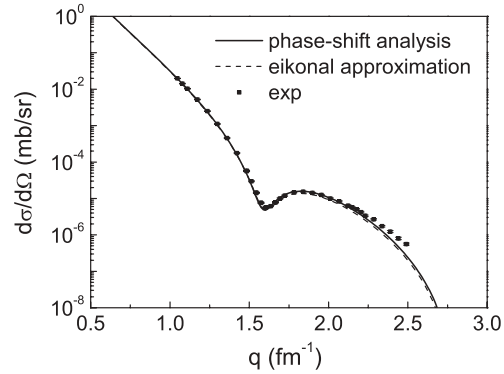

FIG. 6. Elastic electron scattering off ^{16}O at 374.5 MeV.

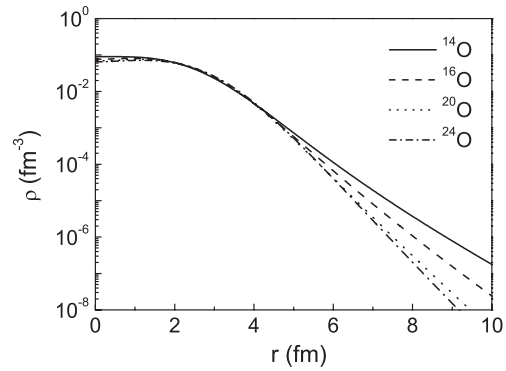

FIG. 7. Nuclear charge densities of O isotopes from RMF theory.

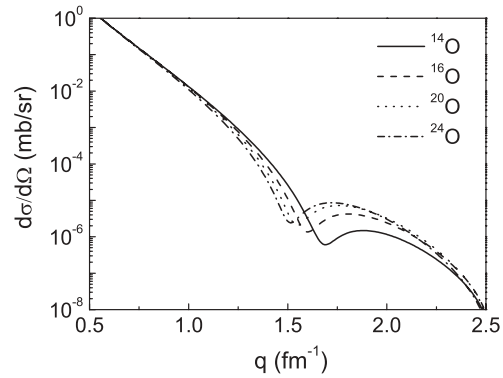

FIG. 8. Elastic electron scattering off O isotopes at 250 MeV.

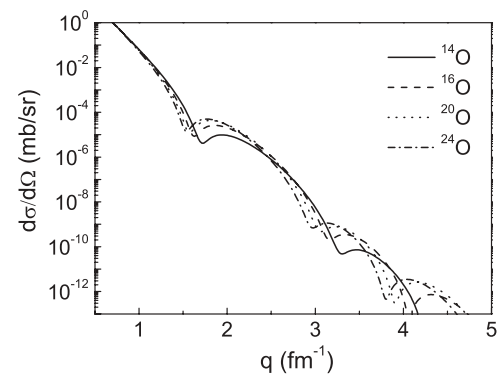

FIG. 9. Elastic electron scattering off O isotopes at 500 MeV.

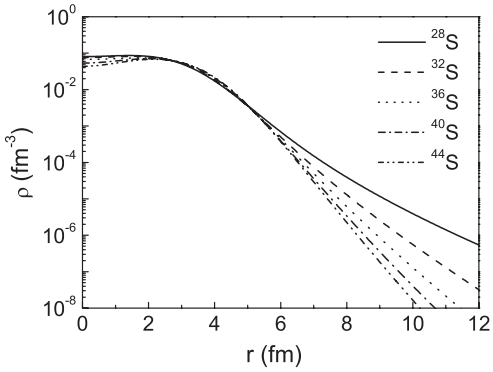

FIG. 10. Nuclear charge densities of S isotopes from RMF theory.

for both light and heavy nuclei. However, with the increase of scattering energy, more and more partial waves have to be taken into account in the calculation. As a result, the calculation becomes more complex, and the physical meaning of the problem becomes so obscure that we cannot see clearly the relation between the cross section and the interaction potential. For high-energy electron scattering, the eikonal approximation is a good choice owing to its physical simplicity and acceptable precision. It connects the differential scattering cross section with the interaction potential in a direct way, as specified in Eqs. (9)–(11). The eikonal approximation is also a very good approximation for high-energy electron scattering off light nuclei, at not very large momentum transfers.

B. Elastic electron scattering off O and S isotopes

In this section, we will study elastic electron scattering off some even-even O and S isotopes with the phase-shift analysis method. These isotopes range from the proton-rich region to the neutron-rich region. In terms of the present experimental situation, it is more likely to reach the dripline in the lighter mass region. Unstable O and S isotopes are the preferential candidates to be produced and investigated in the laboratory. In the following we study elastic electron scattering off the O and S isotopic chains.

The even-even O isotopes are usually expected to be spherical whereas there are different opinions about the shapes of some even-even S isotopes [40–42]. For example, Sarazin

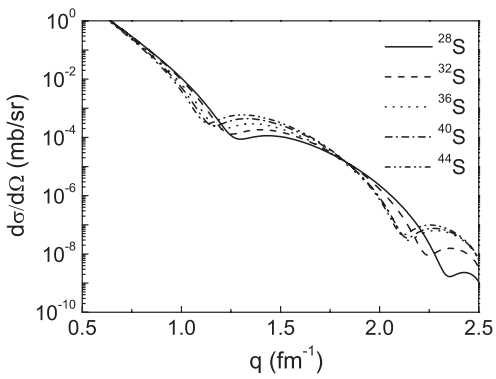

FIG. 11. Elastic electron scattering off S isotopes at 250 MeV.

TABLE II. Theoretical binding energies and rms matter (R_m) and charge ($R_{\rm ch}$) radii of the O and S isotopes. The last column presents the experimental binding energies from Ref. [43].

Isotope	B/A (MeV)	R_m (fm)	$R_{\rm ch}$ (fm)	B/A (MeV) [43]
^{14}O	7.148	2.57	2.74	7.052
^{16}O	8.047	2.61	2.71	7.976
^{20}O	7.690	2.81	2.70	7.569
^{24}O	7.136	3.06	2.74	7.016
^{28}S	7.339	3.05	3.29	7.479
^{32}S	8.234	3.11	3.24	8.493
^{36}S	8.506	3.24	3.27	8.575
^{40}S	8.248	3.35	3.29	8.330
^{44}S	7.956	3.46	3.32	7.994

et al. [42] investigated the properties of S isotopes and concluded that the ground states of some S isotopes are deformed. This is important evidence of the deformation of some S isotopes. In this article, to treat all these nuclei in a consistent way to see the influences of the charge densities on elastic electron scattering, we assume all of the considered isotopes are approximately spherical.

RMF theory is a successful theory that has been widely used for stable and exotic nuclei [44–48]. Here spherical RMF theory with NL-SH parameters is applied to describe these isotopes. The pairing interactions for the open shell nuclei are included in the calculations by the BCS treatment, and the pairing gaps are chosen to be $\Delta_n = \Delta_p = 11.2/\sqrt{A}$ MeV. The nuclear charge densities are obtained by folding the point charge densities and neglecting the contribution from the neutron charge distributions. The proton charge density takes the form $\rho_p(r) = \frac{Q^3}{8\pi} e^{-Qr}$ with $Q = 4.27$ fm^{-1}. Table II shows the basic properties of the O and S isotopes, including the binding energies, the root-mean-square (rms) matter radii, and the rms charge radii. It is seen from Table II that RMF theory can well reproduce the binding energies.

The calculated nuclear charge distributions for these O isotopes are displayed in Fig. 7. With increasing neutron number, skin densities of around $r = 3$ fm increase, while the central and tail densities decrease gradually. The reason for this behavior is that the nuclear potential that the proton feels becomes wider and deeper with increasing neutron number. Thus, on the one hand, the proton density, which is assumed to generate the charge density, is diluted and, as a result, the central charge densities decrease while the skin charge densities around $r = 3$ fm increase. On the other hand, the protons become more bound and the corresponding wave functions at large distances decay more quickly, so the proton or charge densities at large distances decrease more quickly with the increase in neutron number. Having obtained the nuclear charge densities of the O isotopes, we can investigate elastic electron scattering at two typical energies (i.e., 250 and 500 MeV, respectively) to see whether there are observable effects with the increase of neutron number.

Figure 8 shows the differential cross sections of elastic electron scattering off O isotopes at 250 MeV. It is clearly seen that the positions of the first diffraction minimum and maximum shift inward and upward with the increase of the

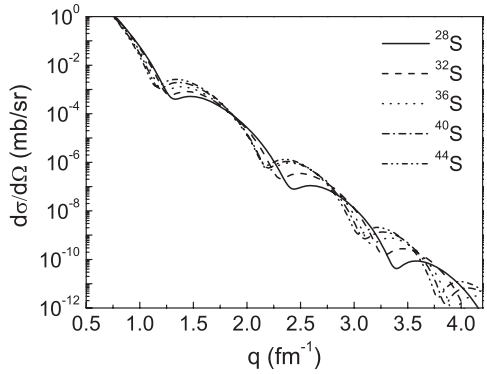

FIG. 12. Elastic electron scattering off S isotopes at 500 MeV.

neutron number. The shift indicates that with the increase of the neutron number the skin charge densities increase and the whole charge density distributions tend to be less extended.

A similar calculation for O isotopes at 500 MeV is shown in Fig. 9. We can also identify the shift of the differential cross section curves with the increase of neutron number.

The charge densities of the S isotopes are shown in Fig. 10. The differential cross sections from S isotopes at 250 and 500 MeV are shown in Figs. 11 and 12, respectively.

According to Figs. 7–12, we can see the influence of the nuclear charge densities on the differential cross sections of elastic electron-nucleus scattering, showing that information about the nuclear charge densities can be deduced from elastic electron-nucleus scattering. Thus, on the one hand, if the cross sections of electron scattering off exotic nuclei can be measured experimentally, the nuclear charge densities can be determined. On the other hand, by comparing the experimental data with the theoretical ones, we can test the validity of RMF theory for exotic nuclei.

IV. SUMMARY

In summary, we have compared the differential electron-nucleus scattering cross sections from two methods: the eikonal approximation and the phase-shift analysis method. Phase-shift analysis is a sophisticated method to calculate the elastic scattering cross section. It has been widely used in elastic electron scattering off both stable and unstable nuclei [28]. The eikonal approximation takes into account the Coulomb distortion effect partially and it is a high-energy approximation for elastic electron scattering [22]. It is simple and direct when used to derive the differential cross section of elastic electron scattering. Comparisons show that the phase-shift analysis can reproduce the experimental scattering data very well in a broad scattering energy range for both light and heavy nuclei. The precision of the eikonal approximation gets better with the increase of the scattering energy, and the eikonal approximation is more suitable for light nuclei. In addition, we have calculated the differential cross sections of elastic electron scattering along the O and S isotopic chains with the phase-shift analysis method. The charge densities of these isotopes are generated from relativistic mean-field theory with NL-SH parameters. The diffraction minima and maxima of the differential cross section curves shift inward and upward with the increase of the neutron number. This shift trend may provide a useful guide for future experimental studies.

ACKNOWLEDGMENTS

This work is supported by the National Natural Science Foundation of China (Grant Nos. 10535010, 10675090, and 10775068), by the 973 National Major State Basic Research and Development of China (Grant No. 2007CB815004), by CAS Knowledge Innovation Project No. KJCX2-SW-N02, and by the Research Fund of Doctoral Point (RFDP), No. 20070284016.

[1] T. W. Donnelly and J. D. Walecka, Annu. Rev. Nucl. Part. Sci. **25**, 329 (1975).
[2] T. W. Donnelly and I. Sick, Rev. Mod. Phys. **56**, 461 (1984).
[3] R. Hofstadter, H. R. Fechter, and J. A. McIntyre, Phys. Rev. **92**, 978 (1953).
[4] R. Hofstadter, B. Hahn, A. W. Knudsen, and J. A. McIntyre, Phys. Rev. **95**, 512 (1954).
[5] R. Hofstadter, Rev. Mod. Phys. **28**, 214 (1956).
[6] H. de Vries, C. W. de Jager, and C. de Vries, At. Data Nucl. Data Tables **36**, 495 (1987).
[7] G. Fricke, C. Bernhardt, K. Heiling, L. A. Schaller, L. Shellenberg, E. B. Shera, and C. W. de Jager, At. Data Nucl. Data Tables **60**, 177 (1995).
[8] I. Angeli, At. Data Nucl. Data Tables **87**, 185 (2004).
[9] A. S. Litvinenko, N. G. Shevchenko, A. Yu. Buki, G. A. Savitsky, V. M. Khvastunov, A. A. Khomich, V. N. Polishchuk, and I. I. Chkalov, Nucl. Phys. **A182**, 265 (1972).
[10] J. L. Friar and J. W. Negele, Nucl. Phys. **A212**, 93 (1973).
[11] I. Sick, Nucl. Phys. **A218**, 509 (1974).
[12] I. Tanihata, Prog. Part. Nucl. Phys. **35**, 505 (1995).
[13] H. Geissel, G. Münzenberg, and K. Riisager, Annu. Rev. Nucl. Part. Sci. **45**, 163 (1995).
[14] A. Mueller, Prog. Part. Nucl. Phys. **46**, 359 (2001).
[15] I. Sick, Prog. Part. Nucl. Phys. **47**, 245 (2001).
[16] T. Suda and M. Wakasugi, Prog. Part. Nucl. Phys. **55**, 417 (2005).
[17] M. Wakasugi, T. Emoto, Y. Furukawa, K. Ishii, S. Ito, T. Koseki, K. Kurita, A. Kuwajima, T. Masuda, A. Morikawa, M. Nakamura, A. Noda, T. Ohnishi, T. Shirai, T. Suda, H. Takeda, T. Tamae, H. Tongu, S. Wang, and Y. Yano, Phys. Rev. Lett. **100**, 164801 (2008).
[18] H. Simon, Nucl. Phys. **A787**, 102 (2007).
[19] An International Accelerator Facility for Beams of Ions and Antiprotons, GSI report, 2006, http://www.gsi.de/GSI-Future/cdr/.
[20] M. E. Rose, *Relativistic Electron Theory* (Wiley, New York, 1961).
[21] D. R. Yennie, D. G. Ravenhall, and R. N. Wilson, Phys. Rev. **95**, 500 (1954).
[22] A. Baker, Phys. Rev. **134**, B240 (1964).
[23] Z. Wang and Z. Ren, Phys. Rev. C **70**, 034303 (2004).
[24] Z. Wang and Z. Ren, Phys. Rev. C **71**, 054323 (2005).
[25] Z. Wang, Z. Ren, and Y. Fan, Phys. Rev. C **73**, 014610 (2006).

[26] A. N. Antonov, M. K. Gaidarov, D. N. Kadrev, P. E. Hodgson, and E. Moya de Guerra, Int. J. Mod. Phys. E **13**, 759 (2004).
[27] A. N. Antonov, D. N. Kadrev, M. K. Gaidarov, E. Moya de Guerra, P. Sarriguren, J. M. Udias, V. K. Lukyanov, E. V. Zemlyanaya, and G. Z. Krumova, Phys. Rev. C **72**, 044307 (2005).
[28] X. Roca-Maza, M. Centelles, F. Salvat, and X. Viñas, Phys. Rev. C **78**, 044332 (2008).
[29] C. A. Bertulani, Phys. Lett. **B624**, 203 (2005).
[30] S. Karataglidis and K. Amos, Phys. Lett. **B650**, 148 (2007).
[31] J. D. Murphy and H. Überall, Phys. Rev. C **11**, 829 (1975).
[32] J. D. Bjorken and S. D. Drell, *Relativistic Quantum Mechanics* (McGraw-Hill, New York, 1964).
[33] L. Schiff, *Quantum Mechanics* (McGraw-Hill, New York, 1968).
[34] F. Salvat, A. Jabalonski, and C. J. Powell, Comput. Phys. Commun. **165**, 157 (2005).
[35] J. B. Bellicard and K. J. van Oostrum, Phys. Rev. Lett **19**, 242 (1967).
[36] J. L. Friar and J. W. Negele, Nucl. Phys. **A212**, 93 (1973).
[37] V. M. Khvastunov, N. G. Afanasyev, V. D. Afanasyev, I. S. Gulkarov, A. S. Omelaenko, G. A. Savitsky, A. A. Khomich, N. G. Shevchenko, V. S. Romanov, and N. V. Rusanova, Nucl. Phys. **A146**, 15 (1970).
[38] G. C. Li, M. R. Yearian, and I. Sick, Phys. Rev. C **9**, 1861 (1974).
[39] I. Sick and J. S. McCarthy, Nucl. Phys. **A150**, 631 (1970).
[40] P. Möller, J. R. Nix, W. D. Myers, and W. J. Swiatecki, At. Data Nucl. Data Tables **59**, 185 (1995).
[41] T. Siiskonen, P. O. Lipas, and J. Rikovska, Phys. Rev. C **60**, 034312 (1999).
[42] F. Sarazin, H. Savajols, W. Mittig, F. Nowacki, N. A. Orr, Z. Ren, P. Roussel-Chomaz, G. Auger, D. Baiborodin, A. V. Belozyorov, C. Borcea, E. Caurier, Z. Dlouhy, A. Gillibert, A. S. Lalleman, M. Lewitowicz, S. M. Lukyanov, F. de Oliveira, Y. E. Penionzhkevich, D. Ridikas, H. Sakuraï, O. Tarasov, and A. de Vismes, Phys. Rev. Lett. **84**, 5062 (2000).
[43] G. Audi, A. H. Wapstra, and C. Thibault, Nucl. Phys. **A729**, 337 (2003).
[44] C. J. Horowitz and B. D. Serot, Nucl. Phys. **A368**, 503 (1981).
[45] B. D. Serot and J. D. Walecka, Adv. Nucl. Phys. **16**, 1 (1986).
[46] Y. Sugahara and H. Toki, Nucl. Phys. **A579**, 557 (1994).
[47] Z. Ren, W. Mittig, B. Chen, and Z. Ma, Phys. Rev. C **52**, R20 (1995).
[48] Z. Ren, W. Mittig, and F. Sarazin, Nucl. Phys. **A652**, 250 (1999).